Is the reaction rate coefficient for $OH+HO_2 \rightarrow H_2O+O_2$ dependent on water vapor?

William H. Brune[1,*] *and Jena M. Jenkins*[1]

[1] Department of Meteorology and Atmospheric Science, Pennsylvania State University, University Park, PA, 16802, USA.

[*]Corresponding author email address: whb2@psu.edu

KEYWORDS: hydroxyl, hydroperoxyl, reaction rate coefficient

ABSTRACT A critical reaction affecting the oxidation chemistry in the middle-to-upper atmosphere occurs between hydroxyl (OH) and hydroperoxyl (HO_2). The reaction rate coefficient for $OH + HO_2 \rightarrow H_2O + O_2$, here called k_{OH+HO2}, has challenged laboratory kineticists for 50 years. However, several measurements from the past 30 years had approached a rough consensus – until the publication of a new study examined, for the first time, the water vapor dependence of this reaction. According to the study, k_{OH+HO2} is not the recommended value of 11.0×10^{-11} cm^3 molec^{-1} s^{-1}, but instead a water-dependent (~1×10^{-11} +2.17×10^{-28}[H_2O]) cm^3 molec^{-1} s^{-1}. Our study examines the water dependence of k_{OH+HO2} using water vapor photolysis of moist air at atmospheric pressure in a flow tube, with direct detection of both OH and HO_2. Observed OH decays were due only to the OH reaction with HO_2 and to a lesser extent the OH loss to the flow tube wall and trace impurities. The resulting k_{OH+HO2} is $(8.54\pm2.90)\times10^{-11}$ cm^3 molec^{-1} s^{-1}, 68% confidence, independent of water vapor and lower than but consistent with the recommended value.

1 Introduction

The atmosphere's primary oxidant, the hydroxyl radical (OH), comes from solar radiation dissociating ozone (O_3) into molecular oxygen (O_2) and excited-state O ($O(^1D)$), which then reacts with water vapor (H_2O) to produce 2 OH molecules. OH then reacts with hundreds of chemical species, often producing the hydroperoxyl radical (HO_2). HO_2 reactions with nitric oxide (NO) or O_3, producing OH. Because the reactions lead to rapid cycling between OH and HO_2, the sum of them, OH+HO_2, is often called HO_x. This cycling continues until HO_2 or OH termination reactions form more stable chemical species. One of the most important termination reactions is R1:

$$OH + HO_2 \rightarrow H_2O + O_2 \qquad \text{(R1)}$$

This reaction terminates both OH and HO_2, returning the radicals to water vapor.

This reaction influences atmospheric chemistry in several ways. First, throughout most of the troposphere, away from urban areas and other large NO sources, this reaction removes from the troposphere a sizeable amount of HO_x, about 15% near Earth's surface, growing to ~50% above 10 km altitude.[1] Second, extreme amounts of OH and HO_2 were recently found to be produced directly by lightning and weaker electrical discharges in thunderstorm outflow anvil clouds.[2] This lightning-generated OH, called LOH, is calculated to be responsible for 2 to 16% of global OH oxidation, but this calculation depends heavily on the reaction rate coefficient of $OH + HO_2 \rightarrow H_2O + O_2$, here called k_{OH+HO2}. This reaction removes over half of the OH before it can react with carbon monoxide (CO) or other chemical species. Thus, the value of the reaction rate

coefficient is critical for determining the atmosphere's oxidation capacity and thus lifetimes of CO, methane (CH_4), and other atmospheric constituents.

The value of the reaction rate coefficient recommended by IUPAC[3] for the reaction of $OH + HO_2 \rightarrow H_2O + O_2$ is

$$k_{OH+HO2}^{IUPAC} = 4.8 \times 10^{-11} \exp(250/T)\ cm^3 molecule^{-1} s^{-1}$$

where T is temperature. At T = 298 K, k_{OH+HO2}^{IUPAC} = 11.0×10^{-11} cm^3 molec^{-1} s^{-1}. This recommendation is based on six studies that measured OH and in some cases also HO_2.[4-9] Two early studies that estimated $OH + HO_2 \rightarrow H_2O + O_2$ by looking at effects of secondary chemistry on the reactions of OH with either hydrogen peroxide (H_2O_2) or ozone (O_3) found rate coefficients of $(1-3) \times 10^{-11}$ cm^3 molec^{-1} s^{-1}.[10,11] A 2020 study by Assaf and Fittschen[12] using direct measurements of OH and HO_2 measured 10.2×10^{-11} cm^3 molec^{-1} s^{-1}, consistent with the IUPAC recommendation. None of these studies examined the reaction rate coefficient as a function of water vapor over a substantial range.

A 2023 study did. Speak et al.[13] used two different laboratory systems and theoretical calculations to study k_{OH+HO2} and its water dependence. They determined the k_{OH+HO2} to be $\sim 1 \times 10^{-11}$ cm^3 molec^{-1} s^{-1} when water vapor was ~10^{16} cm^{-3}, increasing to 8×10^{-11} cm^3 molec^{-1} s^{-1} when water vapor was greater than 3×10^{17} cm^{-3}. The water vapor dependence was determined to be 2.17×10^{-28} cm^6 molec^{-1} s^{-1}. If this result is correct, then OH in the upper troposphere and the impact of lightning-produced OH on global OH oxidation would need to be reassessed.

In response to the Speak et al.[13] results, Chen et al.[14] used the same method as Assaf and Fittchen[12] for determining k_{OH+HO2}, but this time, did the experiments with either no added water vapor or $[H_2O] = 6.32\times10^{16}$ cm^{-3}. In both cases, they obtained $k_{OH+HO2} = (11.0\pm0.12) \times 10^{-11}$ cm^3 $molec^{-1}$ s^{-1}, indicating that k_{OH+HO2} is independent of water vapor.

In this paper, we examine the reaction rate coefficient for $OH + HO_2 \rightarrow H_2O + O_2$ and its water vapor dependence over a range of water vapor concentrations using the simplest, near-atmospheric-like chemistry we could imagine. It involves flowing mixtures of atmospheric pressure air and water vapor past a moveable ultraviolet radiation source and detecting both OH and HO_2 at the end of the flow tube. By varying the water vapor concentrations and HO_x production and directly measuring the OH and HO_2 decays, we were able to determine the k_{OH+HO2} and its water vapor dependence. We compare and contrast our results with those of the previously mentioned references.

2. Experimental design and execution

Our experiments use the discharge-flow method for measuring the decay of OH in the presence of excess HO_2. Details of this apparatus can be found in Jenkins et al.[15] Relevant details for this study are in Table 1. The experimental apparatus consists of a flow tube used primarily for research on OH, HO_2, NO, NO_2, O_3, and other products of electrical discharges including sparks and corona. However, instead of a fixed discharge to create OH and a moveable one for HO_2 as has been used before[7], a moveable mercury (Hg) lamp, positioned just above the quartz flow tube, emits both the 185 nm and 254 nm radiation to create both OH and HO_2 in a disc filling the flow tube cross section and ~1 cm thick along the tube length. Less than 20% of the 185 nm radiation is absorbed even at the tube bottom, resulting in a fairly uniform distribution of

OH and HO_2 throughout the tube's cross-section. Both OH and HO_2 were measured by the Ground-based Hydrogen Oxides Sensor (GTHOS), with its inlet sampling from the center of the flow at the end of the flow tube. [15,17]

Table 1. Characteristics of laboratory set-up and experiments.

component	characteristics	uncertainty (68% confidence)
flow tube	material: fused quartz; I.D: 4.6 cm; length: 105 cm	
flow amount	flow: 50 LPM; pressure: 950-1000 hPa; T = 294 K; R_e ~ 1500; measured centerline velocity: 86 cm s^{-1}; Radial flow profile: not quite fully developed laminar flow.	< 5%
stable gases	air (dewpoint:-40°C; CO ~ 20 ppbv; OH reactivity <0.5 s^{-1}); HPLC-grade water (400-15,000 ppmv)	N/A
detection	OH: LIF in 6-hPa detection cell, sampled through 1-mm hole perpendicular to flow and 0.5 cm from flow tube centerline HO_2: $NO+HO_2 \rightarrow OH+NO_2$, OH LIF in detection cell O_3: UV absorption, Thermo 49C H_2O, pressure, temperature: Vaisala HMT310	±20% ±20% ±5% ±5%
signals	OH signal: on-line 5-500 cts s^{-1}; off-line 0.2 cts s^{-1} HO_2 signal: on-line 20-2000 cts s^{-1}; off-line 0.2 cts s^{-1}	
OH/HO_2 source	UV Hg lamp (Atlantic Ultraviolet 16007-V177); placed 0.5 cm above quartz flow tube; 185nm:254nm < 0.1 ; 8mm slit perpendicular to flow; $flux_{254nm} < 10^{15}$ photons cm^{-2} s^{-1};[16] UV varied by covering with FEP sheets (0.12 mm thick)	
OH decays	five 5-cm steps between 15 – 35 cm from HO_x sampling inlet; OH decay found by least-squares fit to log(OH) versus reaction time for each experiment	±20%
wall loss and impurities	OH: 0.9s^{-1}; impurity: 0.35 s^{-1}; total: 1.25 s^{-1} HO_2: <0.3 s^{-1}	±0.3 s^{-1}
initial radical ranges	OH: $3.5\times10^9 – 2.6\times10^{10}$ cm^{-3} HO_2: $7.2\times10^9 – 1.0\times10^{11}$ cm^{-3} O_3: 0-70 ppbv, except 3 experiments at ~120 ppbv	
Number of experiments	OH wall loss: 22 OH + HO_2 rate coefficient: 51	

GTHOS measures OH by laser-induced fluorescence (LIF) in air that was pulled through a 1-mm pinhole past two detection chambers at 6 hPa pressure. OH absorbs the laser radiation in the

$Q_1(2)$ line at 307.9948 nm (called on-line) and its fluorescence was detected by a gated microchannel plate set at right angles to the laser beam and the flow. The laser was pulsed at 3 kHz, has an average power of 0.5-7 mW, and was passed through the air flow 32 times with a multipass cell. For this experiment the laser power was ~1 mW and the beam diameter at the center of the detection cell was ~ 4 mm. To distinguish the OH fluorescence signal from background signals, 25-seconds of on-line were followed by 5 seconds of off-line, with the laser wavelength shifted, alternately, -0.008 nm or +0.008 nm from the on-line wavelength. HO_2 was detected when NO is added upstream of the detection cell and reacts with HO_2 to produce OH, which is detected by LIF.

For each experiment, OH and HO_2 were measured as the UV lamp was moved further away from the GTHOS inlet in five steps, collecting signal for 30-seconds at each step. A linear least-squares fit to the logarithm of these OH data as a function of reaction time gave a slope equal to the OH decay (s^{-1}).

In the flow tube, the stable gas composition is N_2, O_2, and H_2O. Photolysis by the UV lamp initiates fairly simple chemistry, as shown in the following reaction sequence, where "P" indicates HO_x production and "R" indicates OH reactions.

$$H_2O + UV(185nm) + O_2 \rightarrow OH + HO_2 \quad \text{(P1)}$$

$$O_2 + UV(185nm) + 2O_2 \rightarrow O_3 + O_3 \quad \text{(P2)}$$

$$O_3 + UV(254nm) \rightarrow O(^1D) + O_2 \quad \text{(P3)}$$

$$O(^1D) + H_2O \rightarrow OH + OH \quad \text{(P4)}$$

$$OH + O_3 \rightarrow HO_2 + O_2 \quad \text{(R2)}$$

$$OH + OH \xrightarrow{M} HOOH + O_2 \; or \; H_2O + O \quad \text{(R3)}$$

$$OH + (wall\&impurity) \rightarrow \quad \text{(R4)}$$

$$OH + HO_2 \rightarrow H_2O + O_2 \quad \text{(R1)}$$

No reactions with H_2O_2 as a reactant are listed because only small amounts of H_2O_2 would be produced and the modeled H_2O_2 for these conditions does not exceed 5×10^9 cm^{-3}. Thus, the OH+H_2O_2 reaction frequency, with a rate coefficient of $k_{OH+H2O2} = 1.7\times10^{-12}$ cm^3 molec^{-1} s^{-1}, is negligible. With O_3 less than 70 ppbv (1.7×10^{12} cm^{-3}), R2 and R3 affect the OH decays by less than 4%, although their contributions are still subtracted from the calculated decay slopes of individual experiments. More than 95% of each OH decay is due to R1 and R4.

The frequency for R4 is half the total OH decay for $[HO_2]_{initial} < 2\times10^{10}$ cm^{-3}, but shrinks to less than 20% for $[HO_2]_{initial} > 5\times10^{10}$ cm^{-3}. Thus the frequency for R4 is a large enough fraction that it must be quantified and subtracted from the calculated OH decay slope. To measure this frequency, we decreased HO_2 and OH by reducing water vapor and/or UV flux. The lower HO_2 reduced the contributions of R1, R2, and R3 to the OH decays, while maintaining enough OH to measure the OH decay slope.

In these measurements, the contribution of R1 to the OH wall decay slope varied from 10% to 35% if the IUPAC reaction rate coefficient was used. (Note: in the Discussion, we describe the impact of using the reaction rate coefficient from Speak et al.[13] in this analysis.) Once k_{OH+HO2} was found, it was used to correct the wall loss frequency, which was then used to find an updated value of k_{OH+HO2}. The updated k_{OH+HO2} was then used to find a new value for the wall loss frequency. In the second iteration, the new wall loss frequency was less than 1% different from the previous value, so the iterations were stopped and the updated k_{OH+HO2} was adopted as the reported value. The resulting average OH wall loss/impurity frequency is (1.25 ± 0.3) s^{-1}, 68% confidence.

In the experiments to find the loss frequency for the wall loss and impurity, HO_2 increased slightly while OH decreased. HO_x, the sum of OH and HO_2, decreased less than OH, suggesting that some of the OH loss is due to reactions that cycle OH into HO_2. The HO_x decay will not be influenced by reactions with impurities that cycle HO_x between OH and HO_2, but will be influenced by terminal losses of OH and HO_2. From analysis of the HO_x decays, the loss frequency of R4 due to wall loss is ~0.9 s^{-1}, leaving ~0.35 s^{-1} for an impurity reacting with OH to form HO_2. The measured CO accounts for less than half that impurity.

Reaction P1 produces equal amounts of OH and HO_2, but in the ~0.2 s between the GTHOS inlet and the first accessible measuring point, OH had dropped more than HO_2 because of greater wall and impurity losses. On average, for the OH decay measurements, HO_2 started 4 times larger than OH, with a range of 2 to 10, and dropped on average 15% during the experiment, with a range of 0% to 30%. Furthermore, the HO_2 decrease between the first and final steps is within 15% of the OH decrease when it is corrected for wall/impurity loss. This similar decrease indicates that k_{OH+HO2} is removing them both as expected. Thus, although the initial loss of equal amounts of OH and HO_2 by R1 is quadratic, by the time OH and HO_2 are measured, HO_2 is in excess. We can assume the OH decay is pseudo-first-order using the average HO_2 as the excess reactant for each experiment:

$$k_{OH+HO2} = \frac{d\log(OH)/dt - k_{wall} - k_{OH+O3}[O_3]}{[HO_2]_{average}} \quad \text{(E1)}$$

The uncertainty in the derived rate coefficient for k_{OH+HO2} is dictated primarily by the uncertainties in the OH wall loss, the HO_2 measurement, and the uncertainty due to the precision of the measured OH decays. The precision uncertainty is taken as the standard deviation of the

calculated k_{OH+HO2} and is due to variations in the calculated slopes, discussed further in the results. Uncertainties in the reaction frequencies of $OH+O_3$ and OH+OH are small enough to be neglected in this propagation-of-error analysis. Since the fractional uncertainty in k_{wall} is $\pm$0.25, in $[HO_2]_{average}$ is $\pm$0.20, and in the OH decay slope measurement is $\pm$0.20, all at 68% confidence, the resulting uncertainty in k_{OH+HO2} is $\pm$34%, 68% confidence.

This study is the first time this laboratory flow system has been used to measure a reaction rate coefficient. Measuring reaction rate coefficients in a flow tube with these conditions (970 hPa; 86 cm s^{-1}; 4.6-cm diameter) is uncommon. However, the measured radial velocity profile and the centerline velocity are consistent with expectations for flow approaching but not yet at fully developed laminar flow. To test this system, we chose to find the rate coefficients for two reactions: OH with α-pinene and OH with perfluoropropylene (C_3F_6).

For the α-pinene reaction, known amounts of α-pinene (Aldrich, 98% pure) were added to the humidified air in the flow tube using a syringe pump (Chemyx Inc., Fusion 100) to inject α-pinene into a 1 LPM flow, which was added to the main 49 LPM flow in ½" Teflon tubing prior to the air entering the flow tube. The flow-tube pressure was 970 hPa and temperature was 294 K. The α-pinene concentrations in nine experiments ranged from 6.7×10^{10} cm^{-3} to 2.0×10^{11} cm^{-3}, resulting in the range of OH reactivity from this reaction from 3.6 s^{-1} to 10.8 s^{-1}. Other contributors to the OH decay were $OH+HO_2$ (0.8-2.9 s^{-1}) and OH wall/impurity loss (1.25 s^{-1}). Subtracting these additional contributors from the linear-least-squares slope to the OH decay resulted in $k_{OH+AP} = (5.1\pm0.7)\times10^{-11}$ cm^3 $molec^{-1}$ s^{-1}, where the uncertainty is precision only. This result is consistent with the IUPAC rate coefficient of $k_{OH+AP} = 5.4\times10^{-11}$ cm^3 $molec^{-1}$ s^{-1}.[3]

For the C_3F_6 experiments, a few hPa of C_3F_6 was drawn from the gas over liquid C_3F_6 (SynQuest Labs, 98.5% pure) into a stainless steel reservoir, to which ~2000 hPa of high-purity

N_2 (Linde, 99.999% pure) was added. This C_3F_6/N_2 mixture was flowed at rates between 0 and 5 standard cubic centimeters per minute (sccm) into total flow (50,000 sccm), resulting in five values of $[C_3F_6]$ from 0 to 2.2×10^{12} cm^{-3}. Although C_3F_6 can be photolyzed by the 185 nm radiation with an absorption cross section of $\sim10^{-17}$ cm^2,[18] photolysis with the UV flux given in Table 1 would produce a negligible amount (< 2 pptv) of a fluorine radical. Three different combinations of water vapor and UV filters were used to make different amounts of OH and HO_2. Initial OH was $(0.4\text{-}1)\times10^{10}$ cm^{-3} and, for each of the combinations, HO_2 was independent of C_3F_6 and $(1\text{-}2)\times10^{10}$ cm^{-3}. The slope of the OH decay rate versus $[C_3F_6]$ for all sixteen experiments gave a reaction rate coefficient of $(2.10\pm0.30)\times10^{-12}$ cm^{-3} $molec^{-1}$ s^{-1} and the mean of all values with $[C_3F_6] > 0$ is $(2.24\pm0.39)\times10^{-12}$ cm^3 $molec^{-1}$ s^{-1}. This result is consistent with the IUPAC recommendation of 2.18×10^{-12} cm^{-3} $molec^{-1}$ s^{-1}.[3] Our measured rate coefficients for OH with α-pinene and with perfluoropropylene demonstrate that this laboratory flow system is suitable for measuring OH reaction rate coefficients.

For $OH + HO_2 \rightarrow H_2O + O_2$, some OH decays were calculated with a photochemical box model to ensure that the approximations leading to Eq. 1 were valid. The MCMv3.3.1 mechanism[19] was run using the F0AM photochemical box modeling framework.[20] The inputs to the model included the measured values for pressure, temperature, H_2O, O_3, CO, OH wall loss frequency, initial OH, initial HO_2, and calculated k_{OH+HO2}. The model was run for 0.25 seconds and the intermediate steps were saved.

3. Results

We calculated k_{OH+HO2} for each of the fifty-one OH decays. Four typical OH decays out of the fifty-one experiments are shown in Figure 1. The measurements are the markers, the linear

least-squares fits are the colored lines, and the model-calculated OH decays are the gray dashed lines. For these four experiments, the initial OH ranged from 0.7×10^{10} cm^{-3} to 1.3×10^{10} cm^{-3}, but each one has been scaled to the mean value of the four initial points so that the decays from the different experiments can be more easily compared. To the right of the decays are the average HO_2 concentrations for each experiment. The OH decreases from less than a factor of two to a factor of ten. The legend gives the water vapor concentration and number of filters used for each experiment.

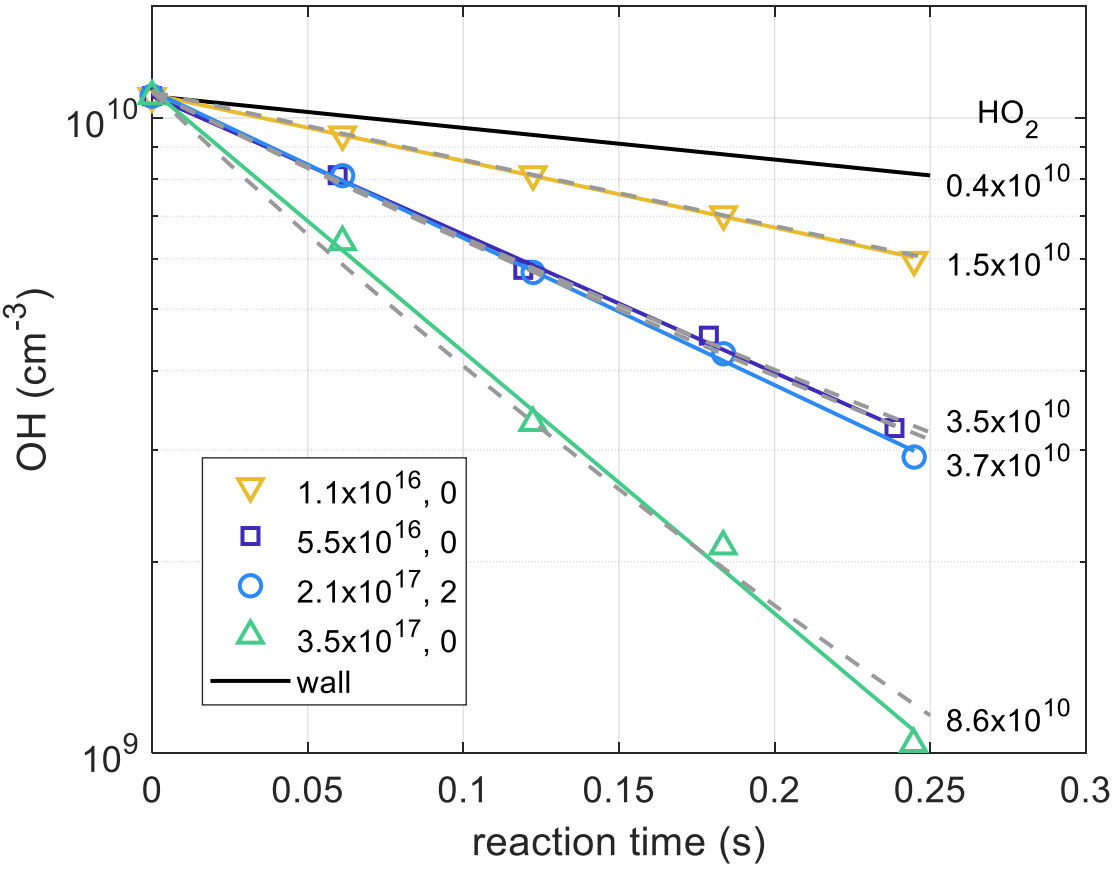

Figure 1. OH decays versus reaction time. Five OH typical decays including wall loss are shown along with their average HO_2 concentrations. Initial OH values have been scaled to the mean

initial value for the plot. The legend shows the water vapor concentration and the number of UV filters used for each experiment. Gray dashed lines show the scaled OH decays as calculated with the MCMv3.3.1 model.

Note the middle two OH decays that are almost identical, as are their average HO_2 concentrations. For the OH decay with $HO_2 = 3.5\times10^{10}$ cm^{-3}, this HO_2 was achieved using 5.5×10^{16} cm^{-3} of water vapor and no filters, while the OH decay with $HO_2 = 3.7\times10^{10}$ cm^{-3} was achieved with 2.1×10^{17} cm^{-3} of water vapor and 2 UV filters reducing the 185 nm radiation. The similarity in these two decays despite the factor-of four difference in water vapor indicates that k_{OH+HO2} is independent of water vapor.

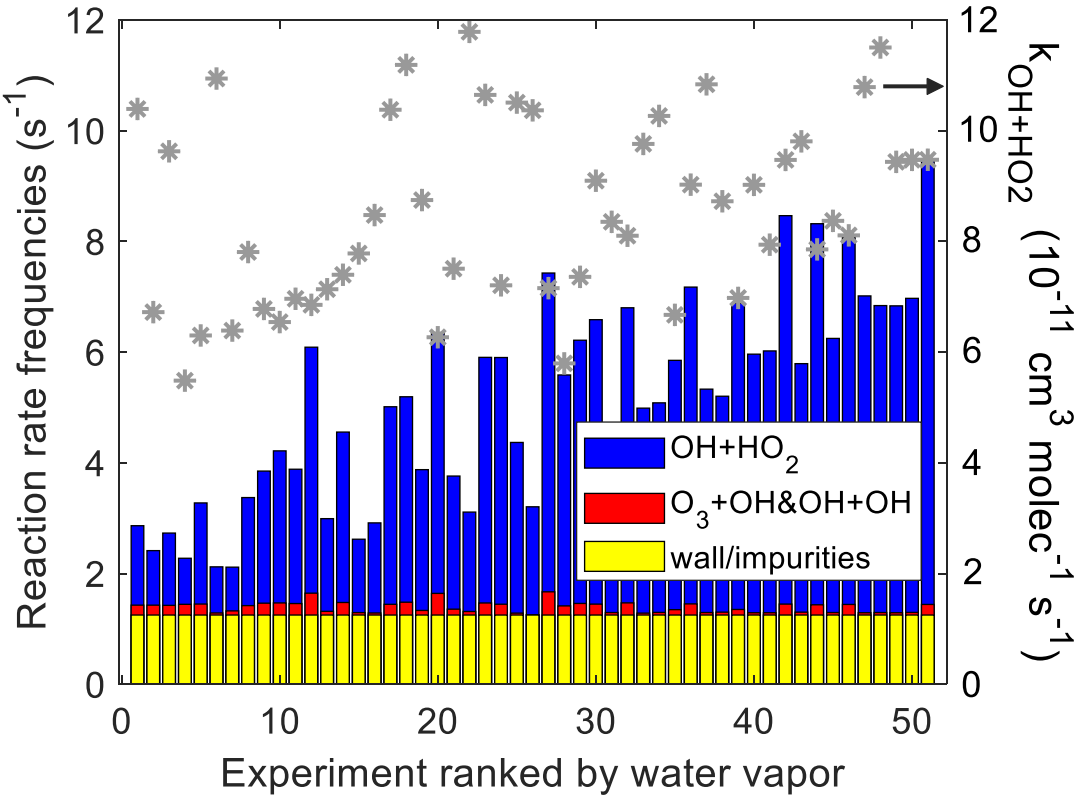

Figure 2. Reaction rate frequencies for the 51 experiments ordered by water vapor. Left axis: Reaction frequencies for $OH+HO_2$ (blue), O_3+OH+OH (red), and wall/impurities (yellow) are shown as bars. Right axis: k_{OH+HO2} for the 51 experiments are given as gray stars.

The reaction frequencies for $OH + HO_2 \rightarrow H_2O + O_2$, the combined reactions of OH with O_3 and OH, and the OH wall loss are shown for the 51 experiments in Figure 2. The experiments are arranged from lowest water vapor to highest. The scatter in k_{OH+HO2} appears to be independent of water vapor, the reaction frequency of $OH + HO_2 \rightarrow H_2O + O_2$, and the difference between the reaction frequency of $OH + HO_2 \rightarrow H_2O + O_2$ and the OH wall loss frequency. Thus the scatter in k_{OH+HO2} is due to other factors, especially statistical variation.

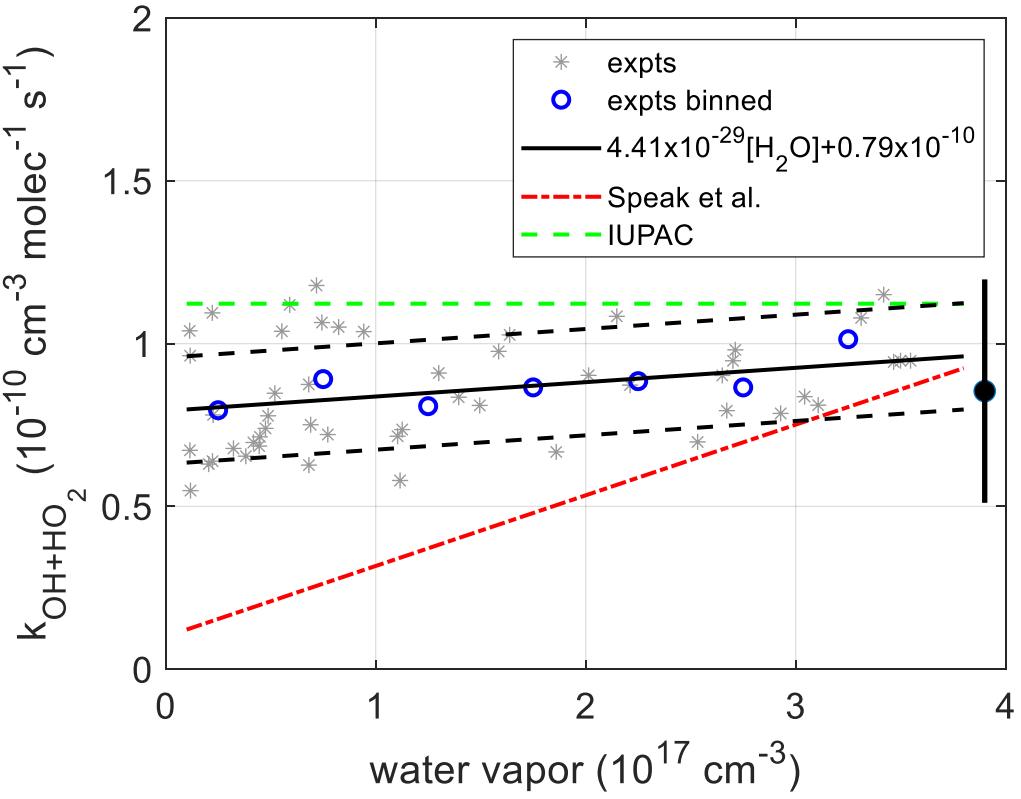

Figure 3. $OH+HO_2$ reaction rate coefficient as a function of water vapor. Shown are the k_{OH+HO2} of all 51 individual experiments (gray stars); the k_{OH+HO2} averaged into 0.5×10^{17} cm^{-3} bins (blue circles); the linear fit to experiments (black line); the standard deviation in k_{OH+HO2} at 68% confidence (dashed black lines); the IUPAC recommendation (green dashed line); and the Speak et al.[13] water-dependent k_{OH+HO2} (red dash-dot line). Average k_{OH+HO2} and its total error (68% confidence) are shown to the right (black dot and lines) and is $(8.54\pm2.90)\times10^{-11}$ cm^3 $mole^{-1}$ s^{-1}.

The reaction rate coefficient k_{OH+HO2} for the 51 experiments are shown in Figure 3. The 51 individual experiments (gray stars) are distributed over the water vapor range, but because the focus of this study was to test the Speak et al.[13] results, half the experiments were conducted at lower water vapor concentrations and thus they have smaller decay slopes and greater statistical variability. Also shown on the figure are k_{OH+HO2} averaged for water vapor bins of 5×10^{16} cm^{-3}, the linear least-squares fit to the 51 experimental results in the solid black line, along with its uncertainty at 68% confidence, dashed lines for k_{OH+HO2} from IUPAC[3] and Speak et al.[13].

4. Discussion

This study has some differences with previous studies. First, in this study all experiments were conducted in air at atmospheric pressure, while most other studies used N_2, Ar, or He as the carrier gas, usually at a lower-than-atmospheric pressures. Second, the reaction frequency range used in this study was ~3-10 s^{-1}, while all other studies had reaction frequency ranges 10 to 100 times larger. Third, the chemistry in this study was designed to minimize all chemical reactions except the reaction of $OH + HO_2$, with OH wall loss/impurity as the only competition. Fourth,

only Speak et al.[13] and this study examine the dependence of k_{OH+HO2} on water vapor over the atmospherically relevant range from ~10^{16} cm^{-3} to ~3×10^{17} cm^{-3}.

In Figure 3, the linear least-squares fit to our experiments has a water vapor dependence of 4.4×10^{-29} cm^6 $molec^{-1}$ s^{-1}, although the slope is not statistically significant. If we assume the slope is real and the water vapor dependence is due to the formation of the HO_2-H_2O complex using the equilibrium constant give in Speak et al.,[13] then the reaction of OH with the complex would need a reaction rate coefficient of ~8×10^{-11} cm^3 $molec^{-1}$ s^{-1}, nearly identical to the water independent intercept for k_{OH+HO2}. Further, the close similarity of the two middle two OH decays in Figure 1, despite the factor-of-four difference in water vapor, provides additional evidence that k_{OH+HO2} calculated from our 51 experiments is independent of water vapor. If Speak et al.[13] was correct, the slopes of these two decays would be different by a factor of 2.5. Thus, our results support a water-independent k_{OH+HO2}, at 68% confidence, of $(8.54\pm2.90)\times10^{-11}$ cm^3 $molec^{-1}$ s^{-1}.

As mentioned in the Experiment design and execution section, the values for OH wall loss are somewhat dependent on the k_{OH+HO2} used to correct the wall loss decays. If the Speak et al.[13] value is used, then the calculated wall loss frequency becomes 1.5 s^{-1}. When this value is used to calculate k_{OH+HO2} from our data as a function of water vapor, $k_{OH+HO2} = 7.4\times10^{-29}[H_2O] + 0.67\times10^{-10}$ cm^{-3} $molec^{-1}$ s^{-1}. As before this water vapor dependence is statistically insignificant and the averaged k_{OH+HO2} is $(7.75\pm2.64)\times10^{-11}$ cm^{-3} $molec^{-1}$ s^{-1}, which is 14% lower than the k_{OH+HO2} we found from these experiments using the IUPAC[3] k_{OH+HO2} to correct the wall loss and 10% lower than the k_{OH+HO2} we found from these experiments using our k_{OH+HO2} to correct the wall loss.

The k_{OH+HO2} from our experiments is lower than but consistent with the IUPAC recommendation and the several studies that support that recommendation[3-9] as well as the more recent studies by Assaf and Fittschen[12] and Chen et al.[14] At water vapor concentrations less than ~2×10^{17} cm^{-3}, our result is inconsistent with the water-dependent result of Speak et al.[13] We have no definitive explanation for this substantial difference with Speak et al.,[13] especially for their theoretical water-dependent result.

The 2016-2018 NASA Atmospheric Tomography (ATom) study was a series of aircraft flights south over the central Pacific Ocean, east over Antarctica, north over in Atlantic Ocean and west over northern Canada, once in each Northern Hemisphere season. These flights consisted of almost constant ascents to 10-14 km followed by descents to ~ 0.2 km, thus scanning almost the entire troposphere. The airborne configuration of GTHOS, called ATHOS, was on these flights.[1] At altitudes above 4 km, water vapor was less than 10^{17} cm^{-3}, and according to Speak et al.,[13] k_{OH+HO2} should be less than 3×10^{-11} cm^3 $molec^{-1}$ s^{-1}. On average for altitudes above 4 km and different latitude bands, the percent difference ($100 \times \frac{observation-model}{(observation+model)/2}$) for OH is less than 30% and for HO_2 is less than 20% for the model using the IUPAC[3] recommendation for k_{OH+HO2}. If the Speak et al.[13] value is used instead, the percent difference is less than that using the IUPAC[3] by as much as 10-15% at some altitudes and latitudes and a similar amount larger for other altitudes and latitudes. In all cases, the percent differences using either Speak et al.[13] or IUPAC[3] are within combined model and observation uncertainty of ~ ±40%. Thus, the ATom results provide no evidence for or against the k_{OH+HO2} from Speak et al.[13]

5. Conclusions

Speak et al.[13] raised an interesting question about the water vapor dependence of the reaction between OH and HO_2. Using our laboratory system designed for electrical discharge studies, we devised flow-tube experiments that measure OH and HO_2 directly in the simplest chemistry we could conceive at atmospherically relevant gas composition and pressure. In the final analysis, these experiments provide substantial evidence that $OH + HO_2 \rightarrow H_2O + O_2$ is independent of water vapor and has a room temperature rate coefficient of $(8.54 \pm 2.90) \times 10^{-11}$ cm^3 $mole^{-1}$ s^{-1}, 68% confidence, lower than but consistent with current IUPAC recommendations[3]. While our result is consistent with the IUPAC recommendation[3], it is ~30% lower and would result in OH being ~5% greater in the upper troposphere and in thunderstorms. We recommend the use of a water vapor independent reaction rate coefficient and the re-evaluation of the IUPAC recommendation[3] considering this new lower k_{OH+HO2}.

SUPPORTING INFORMATION

The following files are available free of charge.

Experimental data used to determine the $OH + HO_2 \rightarrow H_2O + O_2$ reaction rate coefficient. The variables are experiment number, and, for each experiment, pressure, temperature, number concentration, time step for the five OH measurements in each decay, H_2O concentration, number of UV filters, O_3 concentration, HO_2 concentration averaged over the OH decay for each experiment, and OH concentration for each of the five lamp positions in 5-cm increments.

AUTHOR INFORMATION

Corresponding Author

William H. Brune, Department of Meteorology and Atmospheric Science, Pennsylvania State University, University Park, PA, 16803, USA.

Author Contributions

Conceptualization was by W.H.B.. Investigation was by J.M.J. and W.H.B.. Data analysis and modeling was by W.H.B.. Data visualization was by W.H.B.. Manuscript writing of the original draft was by W.H.B.. Reviewing and editing had contributions from J.M.J. and W.H.B..

Funding Sources

Thus study was supported by NSF grant AGS-2323203 and NASA grant 80NSSC19K1590.

ACKNOWLEDGMENT

We thank Y. Yung for calling our attention to Speak et al.[13], P. Stevens for lending us a microchannel plate detector after ours failed, and two anonymous reviewers for their comments.

REFERENCES

1. Brune, W. H.; Miller, D. O.; Thames, A. B.; Allen, H. M.; Apel, E. C.; Blake, D. R., Bui; T. P.; Commane, R.; Crounse, J. D.; Daube, B. C.; et al. Exploring Oxidation in the Remote Free Troposphere: Insights From Atmospheric Tomography (ATom). *J. Geophys. Res.: Atmos.* **2020**, *125,* e2019JD031685*,* DOI: 10.1029/2019JD031685

2. Brune, W. H.; McFarland, P. J.; Bruning, E.; Waugh, S.; MacGorman, D.; Miller, D. O.; Jenkins, J. M.; Ren, X.; Mao, J. and Peischl, J. Extreme oxidant amounts produced by lightning in storm clouds, *Science* **2021**, *372*, 711-715. DOI: 10.1126/science.abg0492

3. Atkinson, R.; Baulch, D. L.; Cox, R. A.; Crowley, J. N.; Hampson, R. F.; Hynes, R. G.; Jenkin, M. E.; Rossi, M. J.; Troe, J. Evaluated kinetic and photochemical data for atmospheric chemistry: Volume I - gas phase reactions of O_x, HO_x, NO_x and SO_x species. *Atmos. Chem. Phys.* **2004**, *4*, 1461−1738. DOI:

4. Braun, M.; Hofzumahaus, A.; Stuhl, F. VUV Flash Photolysis Study of the Reaction of HO with HO_2 at 1 atm and 298 K. *Berichte der Bunsengesellschaft für physikalische Chemie* **1982**, *86***,** 597−602. DOI: 10.1002/bbpc.19820860704

5. Dransfeld, P.; Wagner, H. G. Comparative Study of the Reactions of ^{16}OH and ^{18}OH with $H^{16}O_2$. *Z. Naturforsch., A: Phys. Sci.* **1987**, *42* (5), 471-476. DOI: 10.1515/zna-1987-0508

6. Keyser, L. F. Kinetics of the reaction OH + HO_2 → H_2O + O_2 from 254 to 382 K. *J. Phys. Chem.* **1988,** *92*, 1193−1200. DOI: 10.1021/j100316a037

7. Schwab, J. J.; Brune, W. H.; Anderson, J. G. Kinetics and mechanism of the OH + HO_2 reaction. *J. Phys. Chem.* **1989**, *93*, 1030−1035. DOI: 10.1021/j100340a005

8. DeMore, W. B. Rate constant and possible pressure dependence of the reaction OH + HO_2. *J. Phys. Chem.* **1982**, *86*, 121−126. DOI: 10.1021/j100390a025

9. Cox, R. A.; Burrows, J. P.; Wallington, T. J. Rate coefficient for the reaction OH + HO_2 = H_2O + O_2 at 1 atmosphere pressure and 308 K. *Chem. Phys. Lett.* **1981**, *84*, 217−221. DOI: 10.1016/0009-2614(81)80329-6

10. Wine, P. H.; Semmes, D. H.; Ravishankara, A. R. A laser flash photolysis kinetics study of the reaction OH+H_2O_2→HO_2+H_2O. *J. Chem. Phys.* **1981**, *75*, 4390−4395. DOI: 10.1063/1.442602

11. Chang, J. S.; Kaufman, F. Upper bound and probable value of the rate constant of the reaction OH + HO_2 → H_2O + O_2. *J. Phys. Chem.* **1978**, *82*, 1683−1687. DOI: 10.1021/j100504a003

12. Assaf, E.; Fittschen, C. Cross Section of OH Radical Overtone Transition near 7028 cm^{-1} and Measurement of the Rate Constant of the Reaction of OH with HO_2 Radicals. *J. Phys. Chem. A* **2016**, *120*, 7051−7059. DOI: 10.1021/acs.jpca.6b06477

13. Speak, T. H.; Blitz, M .A.; Medeiros, D. J.; Seakins, P. W. New Measurements and Calculations on the Kinetics of a Old Reaction: OH + HO_2 → H_2O + O_2. *JACS Au* **2023**, *3*, 1684-1694. DOI: 10.1021/jacsau00110

14. Chen, I.-Y.; Chang, C.-W.; Fittschen, C.; Luo, P.-L. Accurate Kinetic Studies of OH + HO_2 Radical−Radical Reaction through Direct Measurement of Precursor and Radical Concentrations with High-Resolution Time-Resolved Dual-Comb Spectroscopy. *J. Phys. Chem. Lett.* **2024**, *15*, 3733-3739. DOI: 10.1021/acs.pjclett.4c00494

15. Jenkins, J. M.; Brune, W. H.; and Miller, D. O. Electrical Discharges Produce Prodigious Amounts of Hydroxyl and Hydroperoxyl Radicals. *J. Geophys. Res.: Atmos.* **2021**, *126*(9), e2021JD034557. DOI: 10.1029/2021JD034557

16. Rowe, J. P., Lambe, A. T. and Brune, W. H. Technical Note: Effect of varying the λ=185 and 254 nm photon flux ratio on radical generation in oxidation flow reactors. *Atmos. Chem. Phys.* **2020**, *20*(21), 13417-13424. DOI: 10.5194/acp-20-13417-2020

17. Faloona, I. C.; Tan, D.; Lesher, R. L.; Hazen, N. L.; Frame, C. L.; Simpas, J. B.; Harder, H.; Martinez, M.; Di Carlo, P.; Ren, X. R.; Brune, W. H. A laser-induced fluorescence instrument for detecting tropospheric OH and HO: Characteristics and calibration. *J. Atmos. Chem.* **2004**, *47*(2), 139-167. DOI: 10.1023/B:JOCH.0000021036.53185.0e

18. Zhang, Z.; Padmaja, S.; Saini, R. D.; Huie, R. E.; Kurylo, M. J. Reactions of Hydroxyl Radicals with Several Hydrofluorocarbons: The Temperature Dependencies of the Rate Constants for $CHF_2CF_2CH_2F$ (HFC-245ca), $CF_3CHFCHF_2$ (HFC-236ea), CF_3CHFCF_3 (HFC-227ea), and $CF_3CH_2CH_2CF_3$ (HFC-356ffa). *J. Phys. Chem.* **1994**, *98*, 4312-4315. DOI: 10.1021/j100067a017

19. Saunders, S. M.; Jenkin, M. E.; Derwent, R. G.; Pilling, M. J. Protocol for the development of the Master Chemical Mechanism, MCM v3 (Part A): tropospheric degradation of nonaromatic volatile organic compounds. *Atmos. Chem. Phys.* **2003**, *3*, 161–180. DOI: 10.5194/acp-3-161-2003

20. Wolfe, G. M.; Marvin, M. R.; Roberts, S. J.; Travis, K. R.; Liao, J. The Framework for 0-D Atmospheric Modeling (F0AM) v3.1. *Geosci. Model Dev.* **2016***, 9*, 3309–3319. DOI: 10.5194/gmd-9-3309-2016